Spatial Structure of a Squeezed Vacuum

L. A. Lugiato and A. Gatti

Dipartimento di Fisica dell' Università di Milano, via Celoria 16, 20133 Milano, Italy

(Received 10 December 1992)

We analyze the quantum properties of the single near field emitted by a degenerate parametric oscillator below threshold, including diffraction and its effects on the threshold for signal generation. The field is probed by a local oscillator field of arbitrary spatial configuration. The results are expressed in terms of an appropriate spectrum which describes how the level of squeezing varies with the angle from the direction of propagation. The results hold for cavities both with plane and with spherical mirrors.

PACS numbers: 42.50.Dv, 42.65.−k

The concept of the squeezed vacuum plays a key role in the field of squeezing, i.e., of the states of the electromagnetic field which present, for the appropriate observables, a level of quantum noise reduced with respect to coherent states. However, the issue of the spatial structure of squeezed vacuum states has not yet been elucidated, mainly because it requires one to combine the field of squeezed states [1] with that of transverse optical patterns [2].

As a matter of fact, the theoretical analyses of squeezed states generation have been performed usually in the plane wave approximation. The exceptions are remarkable but still quite limited in number. Kobolov and Sokolov [3] analyzed the spatiotemporal correlations in the homodyne detection of the field generated by an optical parametric amplifier, and discovered the possibility of photon counting statistics regular not only in time but also in space. La Porta and Slusher [4] studied a parametric amplifier pumped by a Gaussian beam, and predicted limits in the degree of squeezing that arise from spatial distortion of the signal beam. Castelli and one of us [5] considered the quantum properties of the optical spatial patterns which arise spontaneously from diffraction when a Kerr medium contained in a resonant cavity with plane mirrors is driven by a plane wave field, and predicted quantum noise reduction in the intensity difference between the two signal beams which represent the far field configuration of the near field stripe pattern.

In this paper we consider the simplest model of a degenerate optical parametric oscillator (OPO) which includes diffraction and, by introducing appropriate concepts, we provide a description of the spatial structure of the squeezed vacuum state in the near field emitted by this system [1,6]. We derive the formulas which express the quantum fluctuations of the field detected in a balanced homodyne scheme, with a local oscillator field (LOF) of arbitrary spatial configuration. Our results are affected by the instability which gives rise to signal generation. For the appropriate sign of the detuning parameter, the instability threshold is lower for off-axis emission than for axial emission [7]; in this case the signal beam above threshold corresponds to a spatial pattern instead of a plane wave [7].

In this work, however, we consider only the OPO below threshold, in the approximation in which the complete quantum model (including both signal and pump fields) is linearized around the semiclassical stationary solution. In this case, the complete model reduces to a simpler quantum model which involves only the signal field, while the pump field appears only as a classical quantity equal to the stationary semiclassical value.

In the first part of the work we assume that the resonant cavity which contains the nonlinear crystal has plane mirrors. In addition, the coherent driving pump field injected into the cavity has a plane wave structure. We assume conditions such that only one longitudinal mode of the cavity is relevant. In order to avoid difficulties arising from a continuum of transverse modes, we consider in the transverse plane (x,y) a square of side b and we assume periodic conditions for the field. Hence the field envelope operator for the field can be expanded in terms of an orthonormal basis as follows:

$$A(x,y)=\sum_{i=1,2}\sum_{\mathbf{n}} a_{\mathbf{n}i} f_{\mathbf{n}i}(x,y)\,, \tag{1a}$$

$$f_{\mathbf{n}i}=\frac{2^{s_{\mathbf{n}}}}{b}\begin{cases}\cos(\mathbf{k_n}\cdot\mathbf{x}), & \text{for } i=1,\\ \sin(\mathbf{k_n}\cdot\mathbf{x}), & \text{for } i=2,\end{cases} \tag{1b}$$

where $\mathbf{x}(x,y)$, $\mathbf{k_n}=2\pi\mathbf{n}/b$, $\mathbf{n}=(n_x,n_y)$, $n_x=0,1,2,\dots$, $n_y=0,\pm1,\pm2,\dots$, $s_{\mathbf{n}}=(1-\delta_{n_x,0}\delta_{n_y,0})/2$, and the operators $a_{\mathbf{n}i}$, $a^\dagger_{\mathbf{n}i}$ obey the commutation rule $[a_{\mathbf{n}i},a^\dagger_{\mathbf{n}'i'}]=\delta_{\mathbf{n},\mathbf{n}'}\delta_{i,i'}$. In the case $n_x=n_y=0$ only the option $i=1$ is possible.

In the paraxial approximation, in which the transverse components $k_{\mathbf{n}x}$, $k_{\mathbf{n}y}$ of the wave vector are much smaller than the longitudinal component k_z, the frequency of the mode $\mathbf{k_n}$ is given by

$$\omega_k=\omega_0+\frac{ck^2}{2k_z},\quad k=|\mathbf{k_n}|\,, \tag{2}$$

where ω_0 is the frequency of the axial mode $\mathbf{n}=(0,0)$. The k-dependent contribution in Eq. (2) originates from the transverse Laplacian, which describes diffraction and governs the spatial effects in nonlinear optical systems [2].

The model is formulated in terms of a master equation

0031-9007/93/70(25)/3868(4)$06.00

for the density operator ρ of the multimode system. By adopting the picture in which the frequency ω_s of the signal field is eliminated, the master equation reads

$$\frac{d\rho}{dt}=\sum_{i=1,2}\sum_{\mathbf{n}}\Lambda_{\mathbf{n}i}\rho-\frac{1}{\hbar}[H_0+H_{\rm int},\rho]\,, \tag{3}$$

where the Liouvillian $\Lambda_{\mathbf{n}i}$ is given by

$$\Lambda_{\mathbf{n}i}\rho=\gamma_s\{[a_{\mathbf{n}i}\rho,a^\dagger_{\mathbf{n}i}]+[a_{\mathbf{n}i},\rho a^\dagger_{\mathbf{n}i}]\}\,, \tag{4}$$

and γ_s is the cavity damping rate of the signal field. We have, furthermore,

$$H_0=\sum_{i=1,2}\sum_{\mathbf{n}}\gamma_s\Delta_k a^\dagger_{\mathbf{n}i}a_{\mathbf{n}i}\,, \tag{5}$$

$$\begin{aligned}H_{\rm int}&=i\hbar\frac{\bar{A}_P}{2}\int_{-b/2}^{b/2}\int_{-b/2}^{b/2}dx\,dy\{[A^\dagger(x,y)]^2-A^2(x,y)\}\\&=i\hbar\frac{\bar{A}_P}{2}\sum_{i=1,2}\sum_{\mathbf{n}}\{(a^\dagger_{\mathbf{n}i})^2-(a^2_{\mathbf{n}i})\}\,,\end{aligned} \tag{6}$$

where $\Delta_k=(\omega_k-\omega_s)\gamma_s^{-1}$ and $\bar{A}_P$ is the amplitude of the plane wave pump field (taken real and positive for definiteness) multiplied by the coupling constant of the interaction. Thus, the model describes the dynamics of infinite, independent, single-mode degenerate OPO's.

The semiclassical equations for the c-number quantities $\alpha_{\mathbf{n}i}$ and $\alpha^\dagger_{\mathbf{n}i}$ which correspond to the operators $a_{\mathbf{n}i}$ and $a^\dagger_{\mathbf{n}i}$, respectively, read

$$\gamma_s^{-1}\dot{\alpha}_{\mathbf{n}i}=-(1+i\Delta_k)\alpha_{\mathbf{n}i}+A_P\alpha^*_{\mathbf{n}i}\,, \tag{7a}$$

$$\gamma_s^{-1}\dot{\alpha}^*_{\mathbf{n}i}=-(1-i\Delta_k)\alpha^*_{\mathbf{n}i}+A_P\alpha_{\mathbf{n}i}\,, \tag{7b}$$

where $A_P=\bar{A}_P/\gamma_s$. The stationary solution $\alpha_{\mathbf{n}i}=0$ becomes unstable beyond the threshold for signal generation, and the instability is indicated by the fact that some solutions of Eqs. (7a) and (7b) for at least one choice of the indices $\mathbf{n}$ and i diverge for $t\to\infty$. As shown in [7] the instability threshold corresponds to the case $A_P^2=1+\bar{\Delta}_k^2$, where $\bar{\Delta}_k^2$ indicates the minimum value of Δ_k^2 when k is varied from 0 to ∞. Using Eq. (2), one sees that when $\Delta_0\equiv\Delta_{k=0}\geq 0$, the instability arises in the axial mode $\mathbf{n}=(0,0)$ for $A_P^2=1+\Delta_0^2$, whereas when $\Delta_0\leq 0$ the instability arises in the off-axial modes with modulus of the transverse wave vector $k_c=(-2k_z\gamma_s\Delta_0/c)^{1/2}$ for $A_P^2=1$.

In this paper we analyze the quantum properties of the *near field,* immediately out of the cavity. In a balanced homodyne detection scheme (Fig. 1) one observes (see, e.g., [4,8]) the difference between the intensities of the two fields $B_1=(1/\sqrt{2})[A(x,y)+i\alpha_L(x,y)]$ and $B_2=(i/\sqrt{2})[A(x,y)-i\alpha_L(x,y)]$, where $\alpha_L(x,y)$ is the amplitude of the coherent LOF, which has the same frequency of the signal field. The intensity difference corresponds to $N^{1/2}E_H$ where

$$\begin{aligned}&E_H=i(A_H^\dagger-A_H),\quad A_H=G_L[A]\,,\\&N=\int_{-b/2}^{b/2}\int_{-b/2}^{b/2}dx\,dy|\alpha_L(x,y)|^2\,;\end{aligned} \tag{8}$$

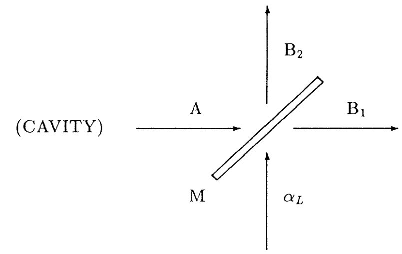

FIG. 1. Balanced homodyne detection scheme. The mirror M has transmission and reflection coefficients $t=1/\sqrt{2}$ and $r=i/\sqrt{2}$, respectively.

here and in the following we indicate by G_L the operation $G_L[f]=N^{-1/2}\int_{-b/2}^{b/2}\int_{-b/2}^{b/2}dx\,dy\,\alpha_L^*(x,y)f(x,y)$. Hence the homodyne detection operates the projection G_L of the field A onto the local oscillator field and selects its quadrature component E_H.

By taking into account that $[A(x,y),A^\dagger(x',y')]=\delta(x-x')\delta(y-y')$ one has that $[A_H,A_H^\dagger]=1$. Possibly, the function $\alpha_L(x,y)$ may also take into account the precise shape of the detected region.

In the observation of squeezing one measures the spectrum of the fluctuations of the homodyne field, which is given by [9]

$$S(\omega)=\mathcal{F}_\omega[\langle:\delta E_H(t)\delta E_H(0):\rangle]\,, \tag{9}$$

where $\mathcal{F}_\omega[g(t)]$ indicates the operation $2\gamma_s\int_{-\infty}^{+\infty}dt\times\exp(-i\omega t)g(t)$, : : means normal and time ordering, $\langle\;\rangle$ denotes the mean value in the stationary state, and $\delta E_H=E_H-\langle E_H\rangle$. With this definition the shot noise level corresponds to $S=0$, and $S(\omega)=-1$ corresponds to complete suppression of quantum noise at frequency ω.

By using Eqs. (8) and (1), we obtain

$$S(\omega)=\sum_{i,i'=1,2}\sum_{\mathbf{n},\mathbf{n}'}\rho_{\mathbf{n}i}\rho_{\mathbf{n}',i'}\mathcal{F}_\omega[\langle:\delta A_{\mathbf{n}i}(t)\delta A_{\mathbf{n}'i'}(0):\rangle]\,, \tag{10a}$$

$$A_{\mathbf{n}i}=i[a^\dagger_{\mathbf{n}i}\exp(i\varphi_{\mathbf{n}i})-a_{\mathbf{n}i}\exp(-i\varphi_{\mathbf{n}i})]\,, \tag{10b}$$

$$\rho_{\mathbf{n}i}\exp(-i\varphi_{\mathbf{n}i})=G_L[f_{\mathbf{n}i}]\,. \tag{10c}$$

The expressions (10) are general and hold whenever the field has the form (1). In the specific case of the model (3) we can take advantage of the fact that the various single-mode degenerate OPOs are independent of one another, i.e., the time correlation function (10a) vanishes unless $\mathbf{n}=\mathbf{n}'$ and $i=i'$. Thus we obtain

$$S(\omega)=\sum_{i=1,2}\sum_{\mathbf{n}}\rho^2_{\mathbf{n}i}S_{\mathbf{n}i}(k,\omega)\,, \tag{11a}$$

$$S_{\mathbf{n}i}(k,\omega)=\mathcal{F}_\omega[\langle:\delta A_{\mathbf{n}i}(t)\delta A_{\mathbf{n}i}(0):\rangle]\,. \tag{11b}$$

It is easy to verify that $\sum_{i=1,2}\sum_{\mathbf{n}}\rho^2_{\mathbf{n}i}=1$. Hence the spectrum $S(\omega)$ is expressed as a combination of spectra (11b) for the individual single-mode degenerate OPOs. These spectra are well known and, indicating $\bar{\omega}=\omega/\gamma_s$, read [10] as

$$S_{\mathbf{n}i}(k,\omega)=4A_P[(1+\Delta_k^2-A_P^2-\bar{\omega}^2)^2+4\bar{\omega}^2]^{-1}\{2A_P-\mathrm{Re}[(1+\bar{\omega}^2-\Delta_k^2+A_P^2-2i\Delta_k)\exp(-2i\varphi_{\mathbf{n}i})]\}\,. \tag{12}$$

Clearly $S(\omega)$ depends on the configuration of the LOF which probes the squeezing properties of the near field. The projection (10c) of the LOF onto the modes $f_{\mathbf{n}i}$ determines both the coefficients $\rho_{\mathbf{n}i}^2$ in the superposition (11a) and the phase $\varphi_{\mathbf{n}i}$ which must be taken in the individual spectra. Let us now focus on the case that the LOF corresponds to a single-mode configuration, i.e., $\alpha_L=N^{1/2}f_{\mathbf{n}i}\exp(i\varphi_{\mathbf{n}i})$, so that $S(\omega)=S_{\mathbf{n}i}(k,\omega)$. If, in addition, the phase $\varphi_{\mathbf{n}i}$ is selected in such a way that the squeezing is optimized for $\omega=0$, i.e., if $\exp(-2i\varphi_{\mathbf{n}i})=(1-\Delta_k^2+A_P^2+2i\Delta_k)[(1-\Delta_k^2+A_P^2)^2+4\Delta_k^2]^{-1/2}$, $S_{\mathbf{n}i}(k,\omega)$ becomes independent of i and equal to

$$S_{\mathrm{opt}}(k,\omega)=\{2A_P-[(1+\Delta_k^2-A_P^2)^2+4A_P^2]^{1/2}-\bar{\omega}^2(1-\Delta_k^2+A_P^2)[(1+\Delta_k^2-A_P^2)^2+4A_P^2]^{-1/2}\}\times 4A_P[(1+\Delta_k^2-A_P^2-\bar{\omega}^2)^2+4\bar{\omega}^2]^{-1}\,. \tag{13}$$

The "continuum" limit $b\to\infty$ can now be taken straightforwardly and Eq. (11a) becomes

$$S(\omega)=\sum_{i=1,2}\int_{-\infty}^{+\infty}\int_{-\infty}^{+\infty}dk_x\,dk_y\,\rho_{\mathbf{k}i}^2 S_i(\mathbf{k},\omega)\,, \tag{14}$$

where $S_i(\mathbf{k},\omega)$ and $\rho_{\mathbf{k}i}$ are still given by Eqs. (12) and (10c), with $\mathbf{n}$ replaced by $\mathbf{k}$, and with the functions $f_{\mathbf{n}i}$ replaced by

$$f_{\mathbf{k}i}=\frac{\sqrt{2}}{2\pi}\begin{cases}\cos(\mathbf{k}\cdot\mathbf{x}), & \text{for } i=1\,,\\ \sin(\mathbf{k}\cdot\mathbf{x}), & \text{for } i=2,\end{cases} \tag{1b$'$}$$

and with the integrals in G_L extended from $-\infty$ to $+\infty$.

Figure 2 shows the behavior of the optimized spectrum (13). This spectrum describes how the squeezing, observed using a single-mode LOF, varies as a function of the transverse wave vector k of the LOF, i.e., how the level of squeezing varies with the angle k/k_z from the direction of propagation [11]. We consider both the resonant case $\Delta_0=0$ [Fig. 2(a)] and the nonresonant case $\Delta_0=-1$ [Fig. 2(b)]; in both cases we focus on the threshold for signal generation $A_P=1$ (of course the threshold case should be considered as the asymptotic limit of the below threshold situation). The complete squeezing occurs at zero frequency for $k=0$ when $\Delta_0=0$ and for $k=k_c$ for $\Delta_0=-1$. Figure 3 details the squeezing at zero frequency, and shows the existence of a range of values for k in which the level of squeezing varies slowly.

Let us now pass to the more realistic case of a cavity with spherical mirrors. For the sake of simplicity, let us assume the following.

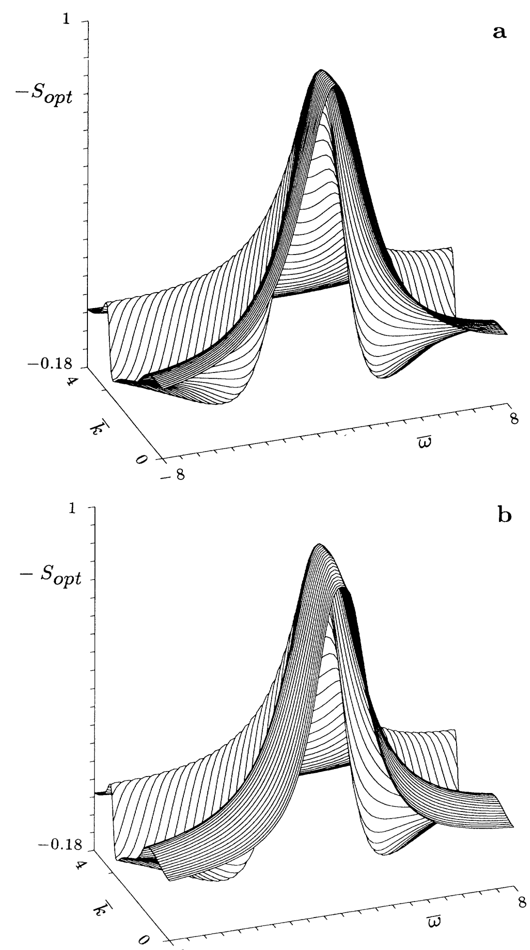

FIG. 2. The spectrum of squeezing (13), with changed sign, is graphed as a function of $\bar{\omega}=\omega/\gamma_s$ and $\bar{k}=k/(2k_z\gamma_s/c)^{1/2}$ at the instability threshold $A_P=1$ for (a) $\Delta_0=0$ and (b) $\Delta_0=-1$.

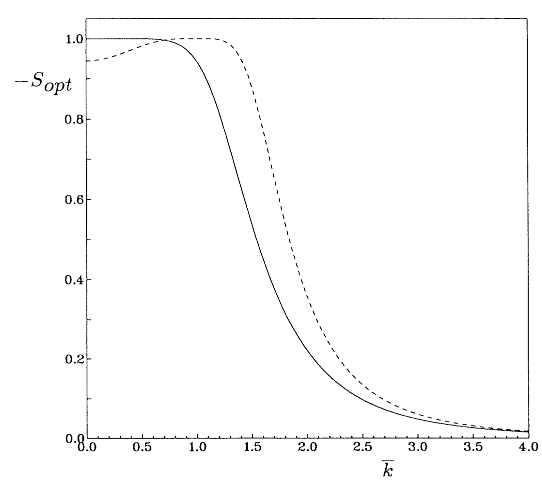

FIG. 3. The curves show the spectrum of squeezing (13) for $\omega=0$, with changed sign, as a function of $\bar{k}=k/(2k_z\gamma_s/c)^{1/2}$ for the same values of the parameters as Fig. 1; solid line: $\Delta_0=0$; dashed line: $\Delta_0=-1$.

(1) The Rayleigh range of the cavity for the signal field is much larger than the length of the crystal, so that the transverse structure of the Gauss-Laguerre orthonormal modes is given by [12]

$$f_{pli}(r,\varphi)=\frac{1}{(2^{\delta_{l,0}}\pi w)^{1/2}}\left[\frac{p!}{(p+l)!}\right]^{1/2}\left[2\frac{r}{w}\right]^{1/2}L_p^l\left[2\frac{r^2}{w^2}\right]\exp\left[-\frac{r^2}{w^2}\right]\begin{cases}\cos(l\varphi), & \text{for } i=1,\\ \sin(l\varphi), & \text{for } i=2,\end{cases} \tag{15}$$

where $p,l=0,1,2,\ldots,$ $i=1,2,$ r, and φ denote the radial and the angular variables in the transverse plane, w is the beam waist, and L_p^l are the Laguerre polynomials of the indicated indices.

(2) The cavity mirrors are completely transmitting for the pump field, which therefore can be assumed again to have a plane wave configuration.

Under such conditions, the field can be expanded as follows:

$$A(x,y)=\sum_{i=1,2}\sum_{p,l=0}^{\infty}a_{pli}f_{pli}(r,\varphi), \tag{16}$$

with $[a_{pli},a^{\dagger}_{p'l'i'}]=\delta_{p,p'}\delta_{l,l'}\delta_{i,i'}$. The mode frequencies are given by

$$\omega_{pl}=\omega_{00}+(2p+l)\zeta, \tag{2$'$}$$

where the parameter ζ depends on the mirrors' separation and radius of curvature. Equations (3)-(6) remain unchanged provided that the index $\mathbf{n}$ is replaced by pl, ω_0 by ω_{00}, and $ck^2/2k_z$ is substituted by $(2p+l)\zeta$.

By defining the detuning parameter $\Delta_{pl}(\omega_{pl}-\omega_s)\gamma_s^{-1}$ one finds again that for $\Delta_{00}\geq 0$ the instability arises in the fundamental mode $p=l=0$ for $A_P^2=1+\Delta_{00}^2$; for $\Delta_{00}<0$ it arises in the higher order modes such that $(2p+l)\zeta\gamma_s^{-1}=-\Delta_{00}$ for $A_P=1$. The spectrum of the intensity fluctuations of the homodyne near field is given by

$$S(\omega)=\sum_{i=1,2}\sum_{p,l=0}^{\infty}\rho_{pli}^2 S_{pli}(\omega), \tag{17}$$

where

$$\rho_{pli}\exp(i\varphi_{pli})=N^{-1/2}\int_0^{\infty}r\,dr\int_0^{2\pi}d\varphi\, f_{pli}(r,\varphi)\alpha_L^*(r,\varphi) \tag{18}$$

and $S_{pli}(\omega)$ is given by Eq. (12) after replacement of Δ_k by Δ_{pl} and $\varphi_{\mathbf{n}i}$ by φ_{pli}.

The results of (17) and (18) are independent of the position on the longitudinal axis z where the homodyne detection takes place, because the Gauss-Laguerre modes vary with z in the known way and remain orthonormal [12].

In this way, with the exception of the passage to the continuum, the previous results have been generalized to the case of a cavity with spherical mirrors, which lends itself to an experimental observation of the spatial structure of the squeezed vacuum, predicted in this paper. The discussion of the elements which can degrade the level of squeezing in an experiment is beyond the scope of this paper.

Central to our analysis is the idea of using a LOF with arbitrary spatial configuration to explore the spatial properties of the squeezed states. If the LOF has a TEM_{00} structure the squeezing coincides with that predicted by the plane wave theory [10]. If, instead, the LOF has the configuration of a higher order mode, the level of squeezing changes because one probes different directions in the emission. When the detuning parameter Δ_{00} is negative the squeezing is largest in some appropriate off-axial directions, as shown in Figs. 2(b) and (3).

We are grateful to Philippe Grangier for helpful advise. This research was carried out in the framework of the ESPRIT Basic Research Actions 6934 QUINTEC and 71118 TONICS and of the CNR Grant No. 92.01369.ct02.

[1] Special issue on "Squeezed Light," edited by R. Loudon and P. L. Knight, J. Mod. Opt. **34** (June/July 1987); special issue on "Squeezed States of the Electromagnetic Field," edited by H. J. Kimble and D. F. Walls, J. Opt. Soc. Am. B **4** (October 1987); special issue on "Quantum Noise Reduction in Optical Systems/Experiments," edited by C. Fabre and F. Giacobino, Appl. Phys. B **55** (September 1992).

[2] Special issue on "Transverse Effects in Nonlinear-Optical Systems," edited by N. B. Abraham and W. J. Firth, J. Opt. Soc. Am. B **7**, 948–1157 (1990); **7**, 1264–1373 (1990); L. A. Lugiato, Phys. Rep. **219**, 293 (1992).

[3] M. I. Kobolov and I. V. Sokolov, Zh. Eksp. Teor. Fiz. **96**, 1945 [Sov. Phys. JETP **69**, 1097 (1989)]; Phys. Lett. A **140**, 101 (1989); Europhys. Lett. **15**, 271 (1991).

[4] A. La Porta and R. E. Slusher, Phys. Rev. A **44**, 2013 (1991).

[5] L. A. Lugiato and F. Castelli, Phys. Rev. Lett. **68**, 3284 (1992).

[6] L. Wu, H. J. Kimble, J. Hall, and H. Wu, Phys. Rev. Lett. **57**, 2520 (1986).

[7] M. Brambilla, A. Gatti, L. A. Lugiato, C. L. Oppo, and F. Prati (to be published).

[8] R. Loudon and P. L. Knight, J. Mod. Opt. **34**, 709 (1987).

[9] B. Yurke, Phys. Rev. A **29**, 408 (1984); M. J. Collett and C. W. Gardiner, *ibid.* **30**, 1386 (1984); H. J. Carmichael, J. Opt. Soc. Am. B **4**, 1588 (1987).

[10] M. J. Collet and D. F. Walls, Phys. Rev. A **32**, 2887 (1985); C. M. Savage and D. F. Walls, J. Opt. Soc. Am. B **4**, 1514 (1987).

[11] Note that this concept is quite different from the spatiotemporal spectrum defined in Ref. [3].

[12] A. Yariv, *Optical Electronics* (Holt, Rinehart, and Winston, New York, 1985), 3rd ed., p. 32.